Title

HEXIM1 controls P-TEFb processing and regulates drug sensitivity in triple-negative breast cancer

Journal

Molecular Biology of the Cell, 31(17)

ISSN

1059-1524

Authors

Shao, Hengyi

Zhu, Qingwei

Lu, Huasong

et al.

Publication Date

2020-08-01

DOI

10.1091/mbc.e19-12-0704

Peer reviewed

HEXIM1 controls P-TEFb processing and regulates drug sensitivity in triple-negative breast cancer

Hengyi Shao[a,†], Qingwei Zhu[a,†], Huasong Lu[a], Amanda Chang[a], Carol Gao[a], Qiang Zhou[a,*], and Kunxin Luo[a,b,*]

[a]Department of Molecular and Cell Biology, University of California, Berkeley, CA 94720; [b]Life Sciences Division, Lawrence Berkeley National Laboratory, Berkeley, CA 94720

ABSTRACT **The positive transcription elongation factor b (P-TEFb), composed of CDK9 and cyclin T, stimulates transcriptional elongation by RNA polymerase (Pol) II and regulates cell growth and differentiation. Recently, we demonstrated that P-TEFb also controls the expression of EMT regulators to promote breast cancer progression. In the nucleus, more than half of P-TEFb are sequestered in the inactive-state 7SK snRNP complex. Here, we show that the assembly of the 7SK snRNP is preceded by an intermediate complex between HEXIM1 and P-TEFb that allows transfer of the kinase active P-TEFb from Hsp90 to 7SK snRNP for its suppression. Down-regulation of HEXIM1 locks P-TEFb in the Hsp90 complex, keeping it in the active state to enhance breast cancer progression, but also rendering the cells highly sensitive to Hsp90 inhibition. Because HEXIM1 is often down-regulated in human triple-negative breast cancer (TNBC), these cells are particularly sensitive to Hsp90 inhibition. Our study provides a mechanistic explanation for the increased sensitivity of TNBC to Hsp90 inhibition.**

Monitoring Editor
Carl-Henrik Heldin
Ludwig Institute for Cancer Research

Received: Dec 20, 2019
Revised: May 28, 2020
Accepted: Jun 2, 2020

INTRODUCTION

Altered gene expression is a hallmark of cancer and plays a key role in malignant progression. The transcription elongation machinery has been shown to control the expression of a large number of genes involved in cell growth, differentiation, and stem cell self-renewal (Zhou and Yik, 2006). For many such genes, RNA polymerase (Pol) II already exists in their promoter-proximal regions in a paused state bound by two negative factors, NELF and DSIF, before the full induction of expression; and the rate-limiting step for their activation is the release of Pol II from the pause. A central component of the transcription elongation machinery is the positive transcription elongation factor b (P-TEFb). Consisting of CDK9 and cyclin T (CycT), P-TEFb releases Pol II from promoter-proximal pausing by phosphorylating the C-terminal domain (CTD) of Pol II, as well as DSIF and NELF. This leads to the production of full-length mRNA transcripts (Zhou *et al.*, 2012).

P-TEFb can exist in at least three distinct major complexes that collectively constitute a functional network (Ott *et al.*, 2011; Zhou *et al.*, 2012). Most P-TEFb in cells are sequestered in an inactive form in the 7SK small nuclear ribonucleoprotein complex (7SK snRNP). Within this complex, 7SK small nuclear RNA (snRNA) serves as a central scaffold that is stabilized by LARP7 (La-related protein 7; He *et al.*, 2008; Krueger *et al.*, 2008) and MepCE (Methylphosphate capping enzyme) (Jeronimo *et al.*, 2007; Xue *et al.*, 2010). HEXIM1 (hexamethylene bisacetamide inducible protein 1) binds to the 7SK snRNA in the complex and inhibits the CDK9 kinase activity (Yik *et al.*, 2003). In response to a number of stress or growth-stimulating signals, P-TEFb is released from the 7SK snRNP and recruited to the chromatin templates by the bromodomain protein BRD4 to promote transcription of many cellular primary response genes such as *Myc, Fos*, and *JunB* (Jang *et al.*, 2005; Yang *et al.*, 2005). P-TEFb can

This article was published online ahead of print in MBoC in Press (http://www.molbiolcell.org/cgi/doi/10.1091/mbc.E19-12-0704) on June 10, 2020.

†These authors contributed equally to this work.

*Address correspondence to: Kunxin Luo (kluo@berkeley.edu); Qiang Zhou (qzhou@berkeley.edu).

Abbreviations used: AML, acute myeloid leukemia; BRD4, bromodomain protein 4; CML, chronic myeloid leukemia; CTD, C-terminal domain; CycT, cyclin T; 3D lrECM, three-dimensional laminin-rich extracellular matrix; EMT, epithelial–mesenchymal transition; ER, estrogen receptor; GA, geldanamycin; HEXIM1, hexamethylene bisacetamide inducible protein 1; HMBA, hexamethylene bisacetamide; KD, knockdown; LARP7, La-related protein 7; MepCE, methylphosphate capping enzyme; MLL, mixed lineage leukemia; MSI, microsatellite instability; NE, nuclear extract; P-TEFb, positive transcription elongation factor b; PR, progesterone receptor; PyMT, Polyoma middle T; RD, radicicol; RNA, Pol II: RNA Polymerase II; SEC, super elongation complex; 7SK snRNP, 7SK small nuclear ribonucleoprotein complex; snRNA, small nuclear RNA; TCGA, cancer genome atlas; TNBC, triple negative breast cancer.

also exist in a transcriptionally active form in the multisubunit super elongation complex (SEC), which contains mostly fusion partners (e.g., AFF1, AFF4, ELL1, ELL2, ENL, and AF9) of the mixed lineage leukemia (MLL) protein. The SEC is recruited by the HIV-1 Tat protein or MLL-fusion proteins to greatly stimulate transcription of HIV and MLL-target genes, respectively (Mueller *et al.*, 2009; He *et al.*, 2010; Lin *et al.*, 2010; Sobhian *et al.*, 2010; Yokoyama *et al.*, 2010; Lu *et al.*, 2014). The latter leads to some of the most severe forms of childhood leukemia.

P-TEFb and its binding partners have been implicated in human cancer. In addition to the key role of the SEC in leukemogenesis (Mueller *et al.*, 2009; Lin *et al.*, 2010; Yokoyama *et al.*, 2010), BRD4, the chromatin adaptor for P-TEFb, has also been linked to many human cancers, including acute myeloid leukemia (AML), chronic myeloid leukemia (CML), and breast cancer (Blobel *et al.*, 2011; Dawson *et al.*, 2011; Zuber *et al.*, 2011; Winter *et al.*, 2012; Wedeh *et al.*, 2015; Ren *et al.*, 2018). BRD4 has been reported to regulate breast cancer progression by modulating Notch and Wnt5A signaling (Shi *et al.*, 2014; Andrieu *et al.*, 2016). The 7SK snRNP components have also been implicated in human breast cancer. For example, microsatellite instability (MSI)–induced LARP7 frame-shift mutations have been detected in ~35% of breast cancer samples characterized as MSI-high (Mori *et al.*, 2002). Further implying a key role of LARP7 in breast cancer progression, we reported that LARP7 is significantly down-regulated in aggressive human breast cancer tissues, and that this down-regulation resulted in increased breast cancer epithelial–mesenchymal transition (EMT) and metastasis (Ji *et al.*, 2014). Mechanistically, we showed that the decreased LARP7 expression reduced the 7SK snRNP level and redistributed P-TEFb to the SEC, leading to P-TEFb activation and increased transcription of EMT transcription factors to promote breast cancer EMT, invasion, and metastasis (Ji *et al.*, 2014).

Given the above results strongly suggesting that P-TEFb activation plays an important role in promoting breast cancer progression, we predict that other P-TEFb partners may also be implicated in breast cancer. Indeed, another 7SK snRNP subunit, HEXIM1, has also been reported to be down-regulated by estrogens and decreased in breast tumors (Wittmann *et al.*, 2003). HEXIM1 was originally identified as a protein that is induced in vascular smooth muscle cells by hexamethylene bisacetamide (HMBA; Ouchida *et al.*, 2003), an inducer of cell differentiation, and was later found to be a critical component of the 7SK snRNP (Yik *et al.*, 2003; Michels *et al.*, 2004). Overexpression of HEXIM1 in breast cancer cells was found to decrease cell proliferation and anchorage-independent growth (Wittmann *et al.*, 2003). Furthermore, in the murine Polyoma middle T (PyMT) transgenic model of breast cancer, HEXIM1 has been found to suppress metastasis (Ketchart *et al.*, 2013). Finally, HEXIM1 can be recruited to the estrogen receptor target gene promoters to cause repression of estrogen-induced gene expression by tamoxifen (Ketchart *et al.*, 2011). Thus, HEXIM1 is clearly implicated in breast cancer. However, its mechanism of action and in particular whether its effects in breast cancer are dependent on its inhibition of P-TEFb have not been determined.

In this study, we examined the role of HEXIM1 in breast cancer and found that HEXIM1 expression is down-regulated in human triple-negative breast cancer (TNBC). This down-regulation renders TNBC cells particularly sensitive to the inhibition of Hsp90. Hsp90, as a molecular chaperone, is essential for the folding, activation, and turnover of many key regulators of cell growth and survival, including protein kinases and steroid hormone receptors, and also plays an important role in oncogenesis (Whitesell and Lindquist, 2005). Advanced cancer cells often exhibit elevated requirement for Hsp90 function to facilitate tolerance of oncogenic mutations and survival of cancer cells under heightened stress conditions from the microenvironment. Tumor cells often display increased abundance of Hsp90, which subsequently promotes tumor cell survival and transformation through effects on Akt, TNFα, NF-κB, and other oncogene or tumor suppressors, and overexpression of Hsp90 in breast cancer correlates with poor prognosis (Sidera and Patsavoudi, 2014). Interestingly, cancer cells appear to be particularly sensitive to inhibitors of Hsp90. For example, Caldas-Lopes *et al.* have shown that TNBC cells are highly sensitive to Hsp90 inhibition (Caldas-Lopes *et al.*, 2009). Moreover, inhibitors of Hsp90 are in Phase II clinical trials for treatment of several solid tumors including breast cancer, melanoma, prostate cancer, and myeloma (Beliakoff *et al.*, 2003; Solit *et al.*, 2008; Suzuki *et al.*, 2010). However, the molecular mechanism underlying this heightened sensitivity to Hsp90 inhibition has not been defined. Our study showed that the sensitivity of breast cancer cells to Hsp90 inhibition correlates with the levels of HEXIM1 and its ability to regulate CDK9 processing. HEXIM1 forms a complex with P-TEFb that serves as an intermediate to transfer the active P-TEFb from Hsp90 to the 7SK snRNP for its suppression. Down-regulation of HEXIM1 locks CDK9 in the immature state in the Hsp90 complex, rendering cells highly sensitive to Hsp90 inhibitors. Our study has provided a molecular basis for the sensitivity of TNBC to Hsp90 inhibition.

RESULTS

HEXIM1 expression level is reduced in TNBC

To investigate the role of HEXIM1 in breast cancer, we first performed data-mining of two publicly accessible datasets, from which HEXIM1 mRNA levels in different cancer types were derived and analyzed. Analysis of the Cancer Genome Atlas (TCGA) dataset demonstrated that the HEXIM1 level is lower in estrogen receptor (ER)– or progesterone receptor (PR)–negative breast cancers, but is not affected by the HER2 status (Figure 1A). Consistently, HEXIM1 expression was down-regulated in TNBC samples (Figure 1B). Analysis of the Oncomine dataset also indicated that HEXIM1 expression was reduced in TNBC (Figure 1C). Similarly, in a variety of human breast cancer cell lines, when they were normalized to the nontransformed mammary epithelial MCF10A cell line, the HEXIM1 mRNA levels were mostly lower in the TNBC cell lines (e.g., MDA-MB-468, MDA-MB-231, and BT549) than in the non-TNBC cells (Figure 1D). Finally, immunohistochemistry staining of a tissue array containing 71 non-TNBC and 66 TNBC samples of human malignant breast cancer showed that HEXIM1 protein level was also markedly reduced in human TNBC tissues (Figure 1E). These analyses suggest that HEXIM1 is down-regulated in human TNBC.

HEXIM1 KD moderately promotes proliferation and migration of breast cancer cells

We next asked whether reducing the HEXIM1 levels in untransformed mammary epithelial cells would promote transformation and malignant progression. To this end, we knocked down HEXIM1 in MCF10A cells by stably expressing a HEXIM1-specific shRNA (Figure 2A) and examined its effect on cell proliferation, morphological differentiation, and cell migration. HEXIM1 knockdown (KD) had little effect on the proliferation or apoptosis of MCF10A cells (Supplemental Figure S1). When cultured in the three-dimensional (3D) laminin-rich extracellular matrix (lrECM), the control MCF10A cells proliferated and underwent morphological differentiation to form multicellular acinar-like structures with well-defined borders and polarity. The HEXIM1 KD cells also formed acinar structures with proper apical and basolateral polarity, but these acini were much

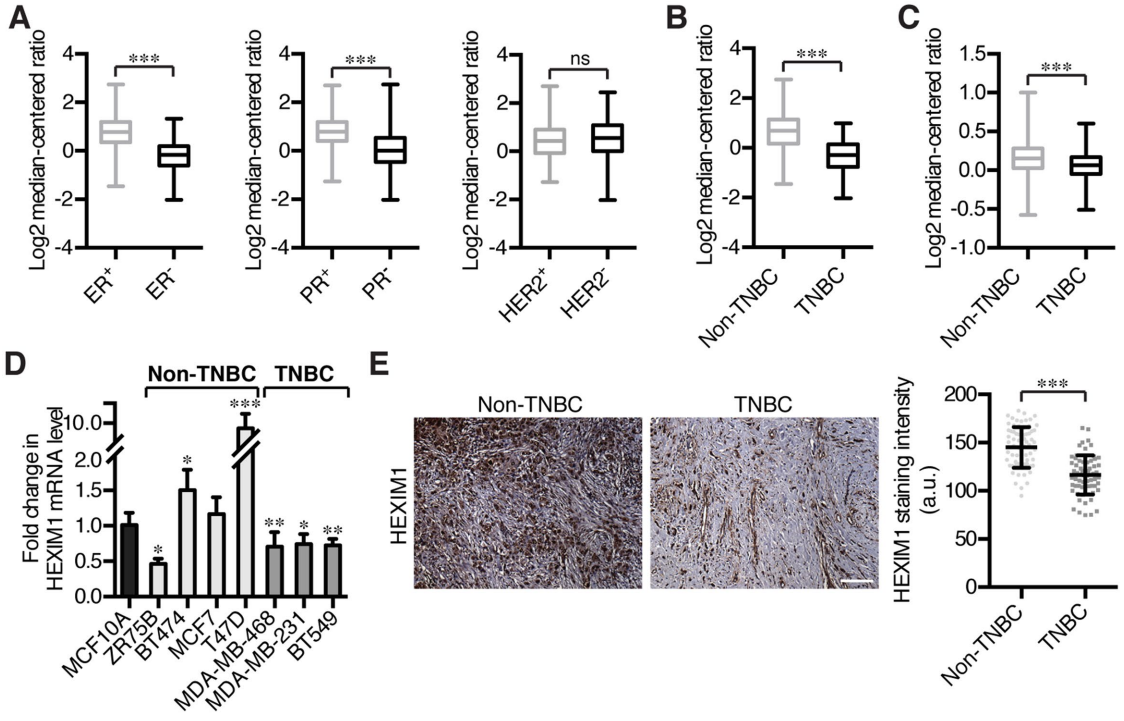

FIGURE 1: HEXIM1 is down-regulated in TNBC. (A) HEXIM1 expression levels in breast cancer of different ER (left), PR (middle), and HER2 (right) status in the TCGA database. ns: not significant, ***$p < 0.001$, Mann–Whitney test. (B, C) Box plots showed the decreased levels of HEXIM1 in TNBC from TCGA, B, and Oncomine, C, databases. ***$p < 0.001$, Mann–Whitney test. (D) HEXIM1 mRNA levels in human breast cancer cell lines as measured by qRT-PCR. PCR values were normalized to that of GAPDH. The HEXIM1 level in the nontransformed MCF10A cells was set as 1. *$p < 0.05$, **$p < 0.01$, ***$p < 0.001$, Student's *t* test. (E) Human breast cancer tissue arrays consisting of malignant non-TNBC samples ($n = 71$) and TNBC samples ($n = 66$) were subjected to IHC staining using anti-HEXIM1. Quantitation of the HEXIM1 level was shown in the graph to the right. Data are shown as means ± SD. ***$p < 0.001$, Student's *t* test. Scale bar: 100 μm.

larger and contained a larger number of cells on the average (Figure 2B). This increase in the size of HEXIM1 KD acini was readily reversed by the reintroduction of HEXIM1-HA (Supplemental Figure S2, A and B). These data suggest that depletion of HEXIM1 leads to an increase in the proliferative potential of cells. This increased proliferation in the 3D culture was not sufficient for oncogenic transformation, as the HEXIM1 KD cells failed to form soft-agar colonies (He *et al.*, 2008).

In both noninvasive T47D and invasive MDA-MB-231 breast cancer cells, HEXIM1 KD moderately enhanced cell motility and migration (Figure 2, C–E), but had little effect on the transforming activity of these cells in vitro as measured by the soft-agar assay for anchorage-independent growth (Figure 2F). Thus, HEXIM1 KD promoted breast cancer cell proliferation and migration, but did not significantly affect the transforming activity of these cells in vitro.

Down-regulation of HEXIM1 sensitizes malignant breast cancer cells to Hsp90 inhibitors

We next examined whether HEXIM1 affected the response of malignant MDA-MB-231 breast cancer cells to chemotherapeutic or other anti-cancer drugs using a colony formation assay to measure cell proliferation and survival in vitro. As shown in Figure 3A, HEXIM1 KD did not change the sensitivity to three chemotherapy drugs, doxorubicin, 5-fluorouracil, and Paclitaxel, which are frequently used in breast cancer treatment. However, the sensitivity to geldanamycin (GA), an Hsp90 inhibitor, was significantly increased. While 4 nM GA only mildly inhibited the colony-forming ability of control MDA-MB-231 cells, it completely suppressed this ability of the two HEXIM1 KD clones (Figure 3B) and caused apoptosis of the treated cells (Figure 3C). Importantly, this enhanced sensitivity to GA in HEXIM1 KD cells could be efficiently reversed by overexpression of an shRNA-resistant HEXIM1-HA cDNA (Supplemental Figure S3, A and B). In addition, the HEXIM1 KD cells showed similarly increased sensitivity to another Hsp90 inhibitor, Radicicol (RD) (Figure 3D). These results suggest that down-regulation of HEXIM1 enhanced the sensitivity of MDA-MB-231 breast cancer cells to Hsp90 inhibition.

A potential correlation between the HEXIM1 levels and the sensitivity to Hsp90 inhibitors seen in MDA-MB-231 cells prompted us to test this correlation further in other breast cancer cell lines. To this end, a panel of breast cancer cell lines expressing varying levels of HEXIM1 was treated with GA and their viability was then assessed. Interestingly, several ER-positive luminal breast cancer cell lines with relatively high expression of HEXIM1, including BT474, MCF7, and T47D, were more resistant to GA than the TNBC cell lines MDA-MB-468 and BT549, which have lower levels of HEXIM1 expression (Figure 3E). One exception is MDA-MB-231, which was more resistant to GA than other TNBC cell lines. We found that although the HEXIM1 mRNA level was low in MDA-MD-231 cells (Figure 1D), the HEXIM1 protein level was relatively high and at a level comparable to those in the ER-positive cell lines (Supplemental Figure S3C). Yet reducing HEXIM1 expression rendered MDA-MD-231 more sensitive to GA (Figure 3, B and C). Consistently, increasing HEXIM1 expression in the HEXIM1-low BT549 cell line rendered the cells less sensitive to GA (Supplemental Figure S3, D and E). Thus, the HEXIM1 level appears to correlate negatively with the sensitivity of

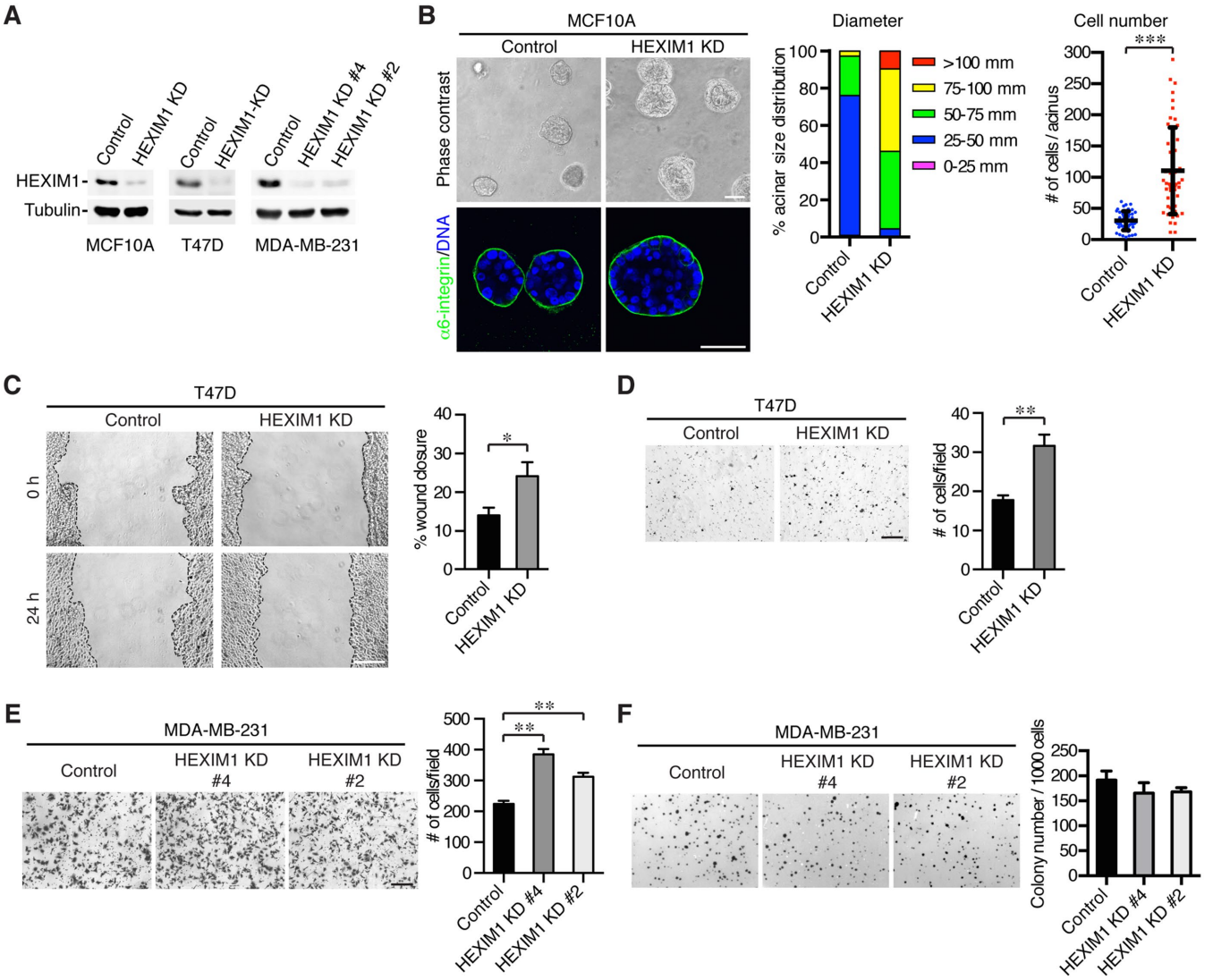

FIGURE 2: HEXIM1 KD moderately promotes breast cancer cell proliferation and migration. (A) Western blotting showing the efficiency of stable HEXIM1 knockdown by shHEXIM1 in MCF10A, T47D, and MDA-MB-231 cells. Tubulin was used as a loading control. (B) Representative phase contrast (top panel) and confocal (bottom panel) images of MCF10A control and HEXIM1 KD cells cultured on lrECM for 7 d. Blue, DAPI; green, α6-integrin. Scale bars: 50 μm. Quantitative analyses of acinar size distribution (middle graph; $n = 110$) and the average cell number per acinus (right graph; $n = 50$) are shown in the graphs. ***$p < 0.001$, Student's t test. (C) Wound healing assay. Wound closure was monitored by phase contrast microscopy and quantified. Data are presented as means ± SEM from four independent assays. *$p < 0.05$, Student's t test. Scale bar: 20 μm. (D, E) Cell migration assay. Transwell assays were performed for 24 h (T47D) or 4 h (MDA-MB-231), and migrated cells were stained and counted. Data are shown as means ± SEM derived from four independent experiments. **$p < 0.01$, Student's t test. Scale bar: 20 μm. (F) Anchorage-independent growth of MDA-MB-231 control or HEXIM1 KD cells was measured by a soft agar assay. The number of colonies was quantified and is shown in the graph to the right.

metastatic breast cancer cells to Hsp90 inhibitors. This result is in agreement with a previous report suggesting that TNBCs are particularly sensitive to inhibition of Hsp90 due to an unknown reason (Caldas-Lopes *et al.*, 2009).

HEXIM1 KD sensitizes xenografted MDA-MB-231 tumors to GA in vivo

Because HEXIM1 KD rendered MDA-MB-231 cells more sensitive to killing by GA, we predicted that GA might also inhibit the oncogenic potential of these cells. Indeed, treatment of MDA-MB-231 HEXIM1 KD cells with GA led to a significant inhibition of the anchorage-independent growth, whereas the same treatment only had a very minor effect on the parental MDA-MB-231 cells (Figure 4A). To examine the effect of GA on tumor growth in a xenograft mouse model in vivo, we injected control MDA-MB-231 cells and their HEXIM1 KD derivative subcutaneously into the nude mice. The HEXIM1 KD was found to promote tumor development markedly, resulting in bigger tumors and an elevated tumor burden (Figure 4, B and C). This is consistent with the model that HEXIM1 has tumor suppressor activities (Wittmann *et al.*, 2003; Ogba *et al.*, 2010; Ketchart *et al.*, 2013; Tan *et al.*, 2016). After the tumors reached a measurable size, the mice were administered GA or vehicle (PBS) for three additional

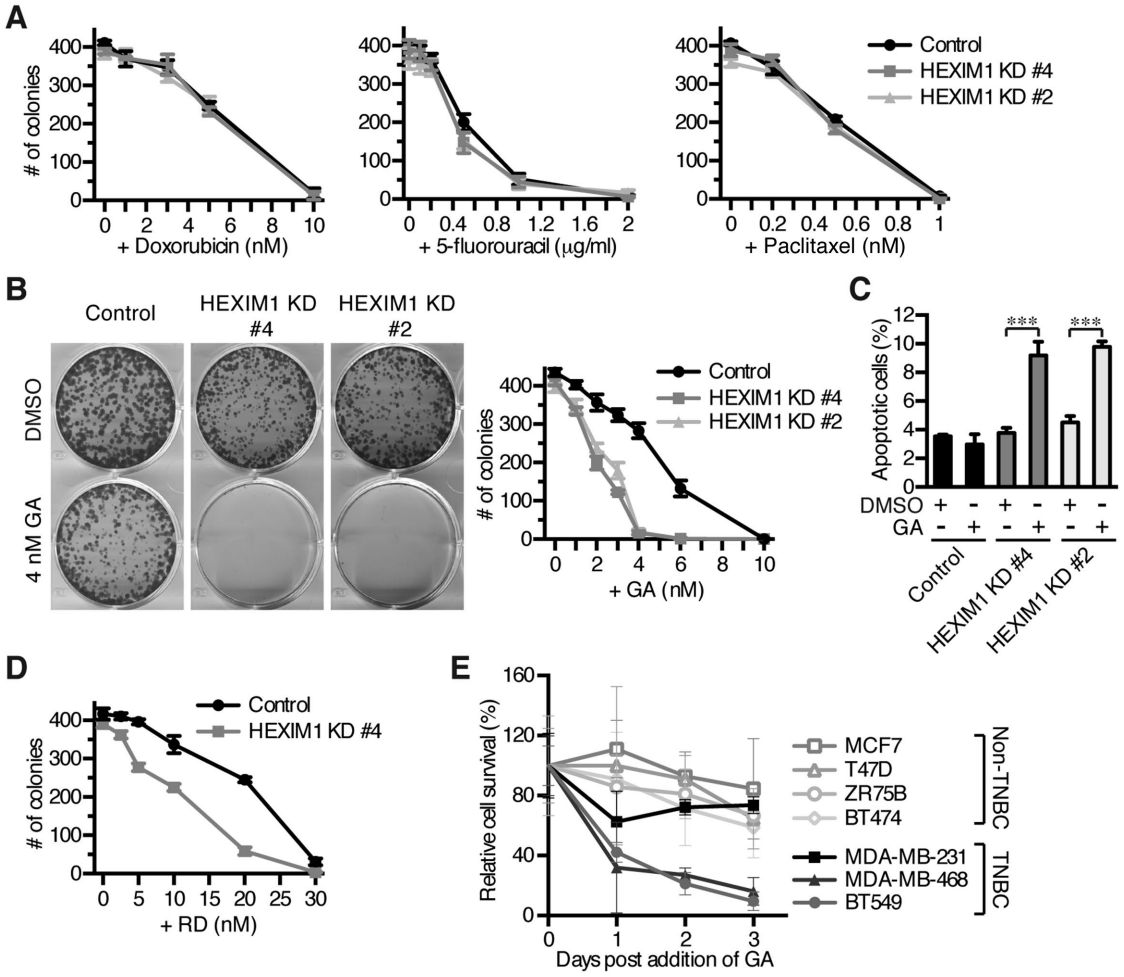

FIGURE 3: HEXIM1 KD increases the sensitivity of metastatic breast cancer cells to Hsp90 inhibitors. (A, B, D) Clonogenic growth assays. MDA-MB-231 control or HEXIM1 KD cells were treated with various concentration of doxorubicin, 5-fluorouracil, or Paclitaxel as indicated in A, GA in B, and RD in D. Representative images of the colony-forming assay are shown in B, and quantitations of the colonies formed are shown in the graphs in A, B, D. (C) Flow cytometric analysis of the apoptotic cells. Cells were treated with GA or DMSO for 48 h, followed by propidium iodide staining and flow cytometric analysis. Data are presented as means ± SD in triplicates. ***$p < 0.001$, Student's *t* test. (E) Viability of various breast cancer cell lines upon treatment with 40 nM GA. The relative cell survival was calculated by comparing the number of cells in GA-treated group to that of DMSO controls. Data represent the average values from three independent assays.

weeks. While GA had little effect on the control tumors, it inhibited growth of the HEXIM1 KD tumors (Figure 4, B and C). Consistently, HEXIM1 KD tumors exhibited a significantly higher level of apoptosis upon GA treatment than control tumors (Figure 4D). Thus, similarly to the observations in vitro, down-regulation of HEXIM1 increased the sensitivity of malignant MDA-MB-231 tumors to Hsp90 inhibition in vivo.

HEXIM1 KD increases binding of CDK9 to Hsp90

We next investigated the mechanism underlying the altered sensitivity of HEXIM1 KD breast cancer cells to Hsp90 inhibitors. Because HEXIM1 is a critical member of the 7SK snRNP that maintains P-TEFb in the inactive state (Yik *et al.*, 2003; Michels *et al.*, 2004), we examined whether the depletion of HEXIM1 redistributed P-TEFb from 7SK snRNP to the active BRD4 or SEC complexes. CDK9 and its associated proteins were isolated by immunoprecipitation with anti-CDK9 antibodies from nuclear extracts of control MDA-MB-231 or HEXIM1 KD cells and analyzed by Western blotting with antibodies targeting different P-TEFb partners. As expected, HEXIM1 KD significantly impaired the assembly of the 7SK snRNP and reduced association of P-TEFb to a key 7SK snRNP component LARP7 (Figure 5A). Surprisingly, HEXIM1 KD also decreased the binding of P-TEFb to the SEC components, including AFF4, ELL2, and to a certain extent ENL, while had little effect on the BRD4-P-TEFb interaction (Figure 5A).

Because there is no free P-TEFb in the cells, and P-TEFb is thought to be maintained in a functional equilibrium among the 7SK snRNP, BRD4-P-TEFb, and SEC complexes, destruction of one such complex is expected to result in P-TEFb's redistribution into the remaining complexes. However, the HEXIM1 KD reduced the bindings of P-TEFb to both 7SK snRNP and the SEC, but did not change the BRD4-P-TEFb interaction. This suggests the possible existence of other protein(s) that may bind to the released P-TEFb.

To determine whether the released CDK9 in HEXIM1 KD cells associated with another cellular protein, we performed affinity purification to identify the CDK9-associated proteins in the HeLa-based

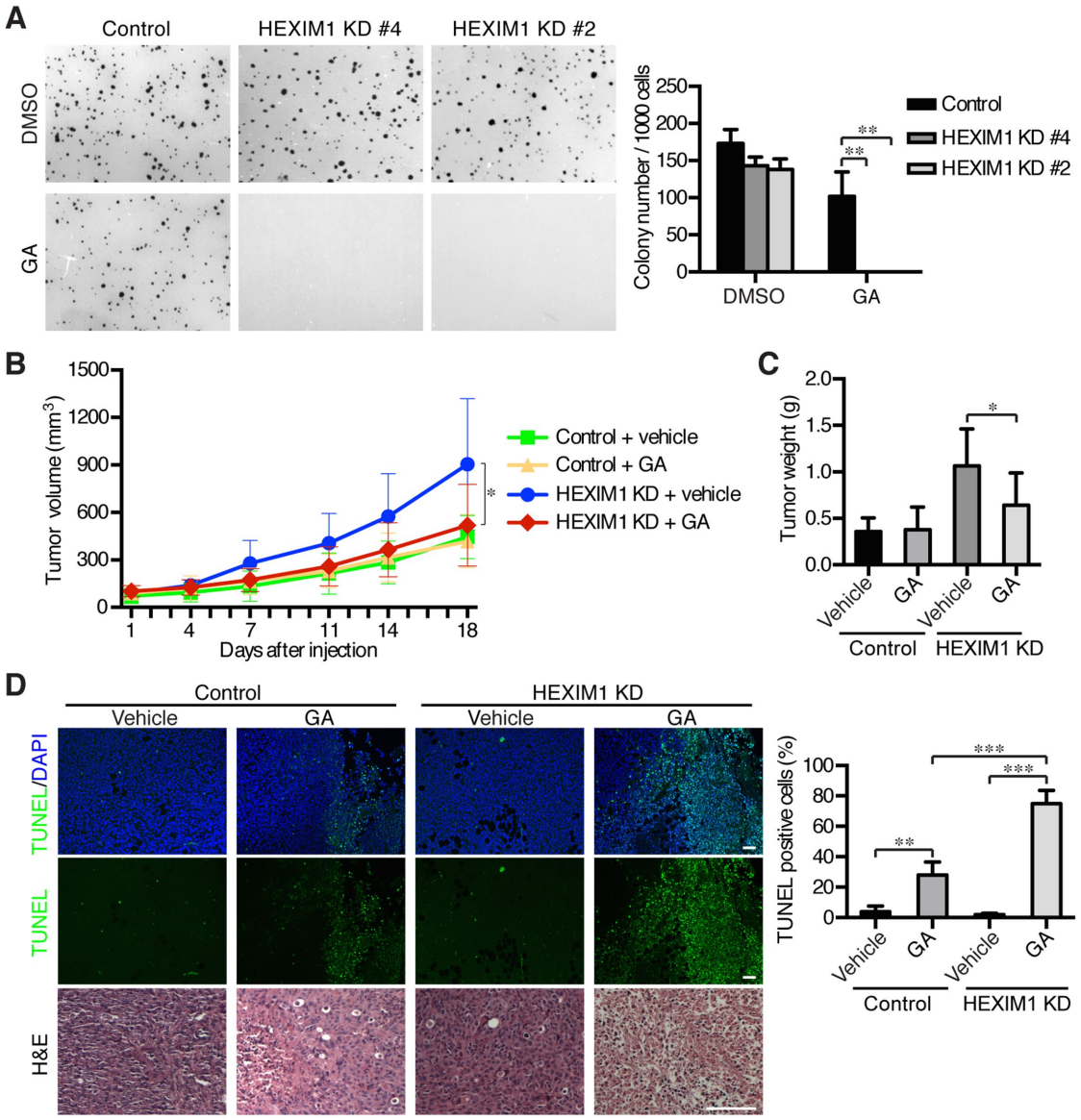

FIGURE 4: HEXIM1 KD sensitizes TNBC tumors to GA in vivo. (A) Soft agar assay. MDA-MB-231 control or HEXIM1 KD cells were grown on soft agar in the presence of 30 nM GA or DMSO. The soft-agar colonies were stained with MTT and quantified and are shown in the right graph. Data are presented as means ± SD in triplicates. $^{**}p < 0.01$, Student's *t* test. (B, C) Effects of GA on breast cancer growth in vivo using the xenograft mouse model. Control or HEXIM1 KD tumors were injected into the nude mice and allowed to grow to approximately 100 mm^3. GA was then injected intraperitoneally twice per week, and tumor volume was measured continuously, B. Tumors were harvested 3 wk later, and tumor weight was measured at the endpoint, C. $^{*}p < 0.05$, Student's *t* test. (D) Tumor sections were subjected to the TUNEL assay and H&E staining. The apoptotic index was calculated as a ratio of the number of apoptotic cells to that of the total cells (right graph). Data are presented as the mean ± SD by Student's *t* test. $^{**}p < 0.01$, $^{***}p < 0.001$. Scale bars: 50 μm.

F1C2 cell line that stably expresses shHEXIM1 and the FLAG-tagged CDK9 (Yang *et al.*, 2001). Similar to the observation in MDA-MB-231 cells, HEXIM1 KD in F1C2 cells also decreased the presence of CDK9 in both the 7SK snRNP and SEC but not in the BRD4 complex (Figure 5B). CDK9-FLAG and its associated factors immunoprecipitated from control and the HEXIM1 KD cells were resolved by electrophoresis and visualized by silver staining (Figure 5C). Interestingly, a protein of approximately 90 kDa was found to interact significantly more with CDK9-FLAG in the KD cells. Mass spectrometry analysis identified this protein as Hsp90. We further confirmed the increased binding of CDK9 to Hsp90 upon HEXIM1 KD using coimmunoprecipitation followed by anti-Hsp90 Western blotting in both MDA-MB-231 and F1C2 background (Figure 5D and Supplemental Figure S4A). Consistent with this, in TNBC cells with a lower HEXIM1 level (MDA-MB-468 and BT549), a notable increase in the CDK9-Hsp90 interaction was detected (Supplemental Figure S4B).

HEXIM1 plays a key role in P-TEFb assembly into the 7SK snRNP

We have previously reported that the newly synthesized CDK9 interacts sequentially with two chaperone proteins in the cytoplasm, Hsp70 and Hsp90, which allows proper folding and assembly of

CDK9 into the active CDK9-CycT1 heterodimer of P-TEFb (O'Keeffe *et al.*, 2000). We showed that inactivation of Hsp90 by GA prevented the generation of active P-TEFb, leading to rapid degradation of the free and unprotected CDK9 (O'Keeffe *et al.*, 2000). To examine whether the increased interaction of CDK9 with Hsp90 upon HEXIM1 KD could be disrupted by GA, the interaction in cells treated with GA or DMSO was assessed by the coimmunoprecipitation assay. As shown in Supplemental Figure S4C, GA abolished the CDK9–Hsp90 interaction in both the HEXIM1 KD and control F1C2 cells, suggesting that the interaction depended on the activity of Hsp90. Consistently, HEXIM1 KD in MDA-MB-231 cells also led to an increase in the CDK9–Hsp90 interaction, which was abolished by GA (Figure 5D). Importantly, this nuclear CDK9-Hsp90 complex is free of Cdc37, which is only detected in the cytoplasmic complex with Hsp90 and CDK9 in transfected 293T cells (O'Keeffe *et al.*, 2000), but not breast cancer cells or Hela cells (Supplemental Figure S4D).

One important question is whether CycT1 is part of the CDK9–Hsp90 complex and whether this Hsp90-bound CDK9 is active as a kinase. The sequential immunoprecipitation assay confirmed that the CDK9–CycT1–Hsp90 complex existed in the HEXIM1 KD cells (Figure 5E), suggesting that the P-TEFb complex is formed in the presence of Hsp90. Furthermore, in an in vitro kinase assay, the Hsp90-bound P-TEFb showed kinase activity comparable to or even higher than that in the CDK9–CycT1 heterodimer, suggesting that the CDK9–CycT1–Hsp90 complex is an active form of P-TEFb (Figure 5F). This explains why in the HEXIM1 KD cells, although the levels of the known SEC-bound P-TEFb complex are decreased, the cells still exhibit active transcription and moderately enhanced oncogenic transformation and invasion. Because P-TEFb is locked into the Hsp90 complex in HEXIM1 KD cells, disruption of this complex by GA results in the accumulation of unprotected CDK9 that is quickly degraded, leading to the depletion of essential P-TEFb from the cells. This could be the underlying mechanism of the observed increased sensitivity of breast cancer cells to the Hsp90 inhibitors. The observation that P-TEFb is stuck in the Hsp90 complex upon HEXIM1 KD also suggests that HEXIM1 is normally required at a step after Hsp90 but before P-TEFb is assembled into the 7SK snRNP for its suppression. Thus, HEXIM1 may form an intermediate complex with CDK9–CycT1 that is required to stabilize and transfer P-TEFb from Hsp90 to the 7SK snRNP. Our study has thus identified the precise step of HEXIM1 action in P-TEFb maturation and suppression.

HEXIM1 KD increases the sensitivity of breast cancer cells to inhibition of CDK9

The above model makes two predictions. First, if the CDK9–CycT1–Hsp90 and CDK9–CycT1–HEXIM1 complexes are necessary key intermediates for P-TEFb maturation before P-TEFb is assembled into the 7SK snRNP, a complete disruption of the Hsp90–P-TEFb complex by GA should result in a decrease in the binding of CDK9 with HEXIM1, as well as its assembly into the 7SK snRNP, even in cells without the HEXIM1 KD. Indeed, when treated with increasing concentrations of GA, a gradual decrease in the associations of CDK9 with HEXIM1 and another key 7SK snRNP component, LARP7, was detected (Figure 5G).

Second, because HEXIM1 KD resulted in an increase of the active Hsp90-P-TEFb complex, these cells should also become sensitive to the inhibition of CDK9. To test this, we treated control and HEXIM1 KD MDA-MB-231 cells with increasing concentrations of iCDK9, a highly selective CDK9 inhibitor (Lu *et al.*, 2015) and examined the inhibitory effects on cell proliferation and survival with the colony formation assay. As shown in Figure 5H, the KD cells exhibited an elevated sensitivity to iCDK9 compared with the control cells. Moreover, a low concentration of iCDK9 (0.02 μM), although by itself it had a very minor effect on the colony formation ability of the cells, caused a slight but consistent enhancement of the suppressive effect of GA on the KD cells (Figure 5I), confirming that the heightened sensitivity of the HEXIM1 KD cells to Hsp90 inhibition is dependent on CDK9 and that the KD sensitizes cells to drugs targeting the P-TEFb–Hsp90 complex.

DISCUSSION

HEXIM1 was previously known as a key component of the 7SK snRNP that functions to inhibit the kinase activity of P-TEFb (Yik *et al.*, 2003; Zhou and Yik, 2006). Here, we show that HEXIM1 is essential for the assembly of P-TEFb into the 7SK snRNP by forming an intermediate complex with P-TEFb that allows transfer of P-TEFb from Hsp90 to 7SK snRNP (Figure 5J). Our data indicate that P-TEFb kinase activation occurs in the Hsp90 complex, and HEXIM1 acts at a step after this activation to enable the assembly of P-TEF into the 7SK snRNP to suppress its kinase activity. Depletion of HEXIM1 not only disrupted the 7SK snRNP, but more importantly, prevented P-TEFb from assembling into the 7SK snRNP and caused accumulation of active P-TEFb in the Hsp90 complex. These active P-TEFb-Hsp90 complexes can activate transcription to promote malignant progression of HEXIM1 KD breast cancer cells and at the same time render these cells more sensitive to the inhibitors of both Hsp90 and CDK9. This model explains well the observed different effects of the KD of LARP7 versus that of HEXIM1 on P-TEFb's kinase activity. LARP7 KD does not affect the earlier steps of P-TEFb maturation and processing, but releases P-TEFb from the 7SK snRNP to form more active SEC and BRD4 complexes (Ji *et al.*, 2014). In contrast, HEXIM1 KD prevented P-TEFb from incorporating into the 7SK snRNP and all the subsequent complexes (SEC and BRD4), and thus locked P-TEFb into the Hsp90 complex. While LARP7-low malignant breast cancer cells are sensitive to CDK9 and BRD4 inhibitors, HEXIM1-low TNBC are more prone to inhibition by Hsp90 and CDK9 inhibitors. Thus, our studies have suggested different treatment options for highly malignant breast cancer with different mutations in the P-TEFb pathway.

Previously, it has been reported that TNBCs are particularly sensitive to inhibition of Hsp90. In addition, PU-H71, another Hsp90 inhibitor that has entered Phase I clinical trial, was shown to be more active in the TNBC than non-TNBC models (Caldas-Lopes *et al.*, 2009). However, the mechanism for this heightened sensitivity has not been defined clearly. Hsp90 is known to affect the activities of many client oncogenic proteins, including PI3K/Akt, JAK/STAT, RAS/ERK, NF-κB, and CDKs, that are involved in various key signaling pathways (Sidera and Patsavoudi, 2014). Thus, the inhibition of Hsp90 could affect tumor proliferation and apoptosis through these pathways. However, these pathways are not unique to TNBC and thus cannot fully explain why TNBC is particularly sensitive to Hsp90 inhibition. Our study here has suggested that the reduced HEXIM1 levels in TNBC and its impact on CDK9 processing and regulation may underlie this sensitivity. We showed that HEXIM1 is down-regulated in TNBC and that this down-regulation results in accumulation of CDK9 in the Hsp90 complex and a significant decrease in the known P-TEFb complexes (SEC and 7SK snRNP) in cells. Hsp90 inhibitors block maturation of CDK9 by disrupting the CDK9–CycT1–Hsp90 complex and thus produce high levels of immature and unprotected CDK9 that are quickly degraded, leading to the depletion of the critically needed P-TEFb in cells, resulting in cell death. Our study has thus provided a mechanistic link between the generally

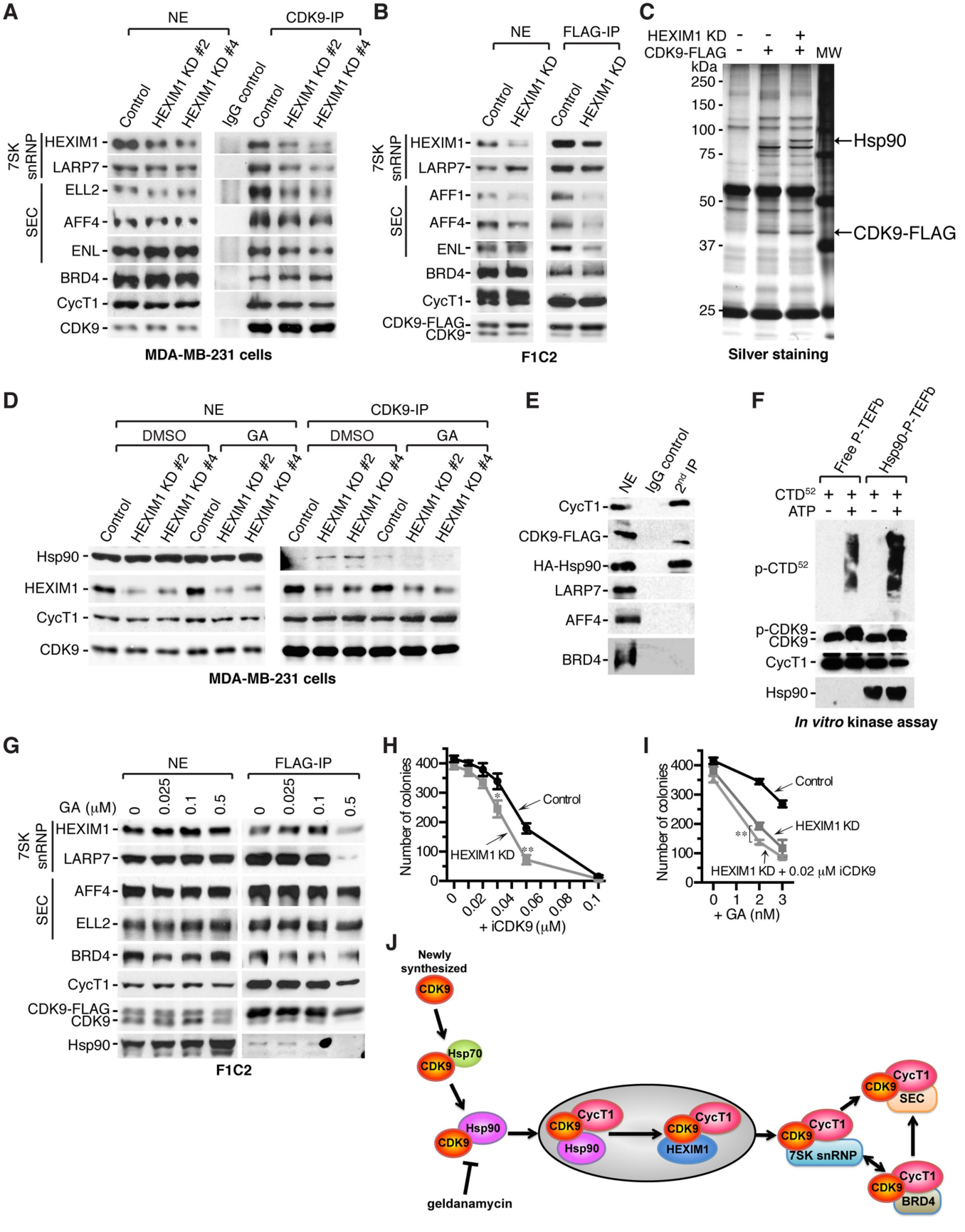
A
NE
CDK9-IP
Control
HEXIM1 KD #2
HEXIM1 KD #4
IgG control
7SK snRNP
SEC
HEXIM1
LARP7
ELL2
AFF4
ENL
BRD4
CycT1
CDK9
MDA-MB-231 cells
B
NE
FLAG-IP
Control
HEXIM1 KD
AFF1
CDK9-FLAG
F1C2
C
HEXIM1 KD
CDK9-FLAG
MW
kDa
250
150
100
75
50
37
25
Hsp90
CDK9-FLAG
Silver staining
D
DMSO
GA
MDA-MB-231 cells
E
NE
IgG control
2nd IP
HA-Hsp90
F
Free P-TEFb
Hsp90-P-TEFb
CTD52
ATP
p-CTD52
p-CDK9
In vitro kinase assay
G
GA (μM)
0
0.025
0.1
0.5
F1C2
H
Number of colonies
Control
HEXIM1 KD
+ iCDK9 (μM)
I
HEXIM1 KD + 0.02 μM iCDK9
+ GA (nM)
J
Newly synthesized
Hsp70
Hsp90
geldanamycin
HEXIM1
7SK snRNP
SEC
BRD4

low HEXIM1 levels in TNBC and the heightened sensitivity of these cells to Hsp90 inhibitors. More importantly, combinatory treatment with both Hsp90 and CDK9 inhibitors show higher efficiency of suppression of TNBC. Thus, our study has revealed a potentially novel and promising therapy for TNBC using the combination of CDK9 with Hsp90 inhibitors.

In addition to its functions in P-TEFb processing and regulation, HEXIM1 has also been reported to play a role in DNA-mediated innate immune response by binding to the NEAT1 long noncoding RNA and forming a multi-subunit RNA-protein complex that includes DNA-PK and other para-speckle factors (Morchikh *et al.*, 2017). It is not clear whether this P-TEFb-independent function of HEXIM1 is related to its role in human cancer, as these HEXIM1-containing RNA–protein complexes are mostly involved in anti-microbial and autoimmune responses and have not been linked to solid human tumors. In contrast, the ability of HEXIM1 to regulate P-TEFb has been implicated in many human cancers, including melanoma (Tan *et al.*, 2016) and breast cancer (Ogba *et al.*, 2010; Ketchart *et al.*, 2011). Thus, the increased sensitivity of TNBC cells to Hsp90 inhibition caused by down-regulation of HEXIM1 is very likely a P-TEFb-dependent process, which also explains the sensitivity of these cells to iCDK9. Because HEXIM1 has also been found to be down-regulated in malignant melanoma (Tan *et al.*, 2016), these tumor cells could also become hypersensitive to inhibitors of Hsp90 and/or CDK9. Indeed, Hsp90 inhibitors have been found to inhibit melanoma proliferation and survival (Yeramian *et al.*, 2016; Calero *et al.*, 2017), enhance immunotherapy (Mbofung *et al.*, 2017), and help overcome the resistance of metastatic melanoma cells to BRAF inhibitors (Paraiso *et al.*, 2012; Smyth *et al.*, 2014). Thus, the HEXIM1-mediated sensitivity to Hsp90 inhibition may be a general phenomenon that can be exploited for the treatment of other metastatic human cancers in addition to TNBC. Our work also implies that the combinatory inhibition of both Hsp90 and CDK9 is a highly effective therapy for treating TNBC and other metastatic tumors.

MATERIALS AND METHODS

Cell lines

The MCF10A mammary epithelial cells were cultured in DMEM-F12 supplemented with 5% horse serum, 20 ng/ml EGF, 10 μg/ml insulin, 0.5 μg/ml hydrocortisone, 100 ng/ml cholera toxin, and 1% penicillin/streptomycin. T47D, BT474, ZR75B, and BT549 cells were maintained in RPMI-1640 media containing 10% FBS. MDA-MB-231, MDA-MB-468, MCF7, and HeLa cells were cultured in DMEM plus 10% FBS. The F1C2 cell line is a HeLa-based cell line stably expressing Flag-tagged CDK9 (Yang *et al.*, 2001).

Antibodies

The antibodies against CDK9, LARP7, HEXIM1 and BRD4 were generated as previously described (Yang *et al.*, 2001, 2005; Yik *et al.*, 2003; He *et al.*, 2008). Anti-AFF1 and ENL antibodies were purchased from Bethyl Laboratories (Montgomery, TX), anti-AFF4 and Hsp90 antibodies from Abcam (Cambridge, UK), CycT1 antibody from Santa Cruz Biotechnology, α6-integrin antibody from Zymed, anti-tubulin from Calbiochem (San Diego, CA), and anti-Flag (M2) from Sigma-Aldrich (St. Louis, MO). Horseradish peroxidase (HRP)–conjugated anti-rabbit and anti-mouse antibodies were from Jackson ImmunoResearch Laboratories and Alexa 488-conjugated anti-rat antibody was from Invitrogen.

Transfection and infection

shRNA targeting human HEXIM1 (sequence: 5′-AAACAGAGCCTTCGAGCTTC-3′) or an shRNA-resistant human HEXIM1-HA (sequence: 5′-AAACAGAGCTTGAGAGCTTC-3′) was introduced into breast cancer cell lines by retroviral infection as described previously (Zhu *et al.*, 2007). Briefly, shHEXIM1 in pSUPER.retro.puro vector or HEXIM1-HA in pBabe.puro vector was transfected together with retroviral packaging vectors into 293T cells, and viral supernatant was used to infect the breast cancer cells. Single colonies of infected cells were selected in the presence of puromycin and analyzed.

Quantitative RT-PCR (qRT-PCR)

qRT-PCR was performed with ABI 7300 (Applied Biosystem) and a DyNAmo HS SYBR Green qPCR kit (Fisher Scientific) according to the manufacturers' instructions. The gene-specific primers used in qRT-PCR are HEXIM1, forward 5′-CCAGCCTCAAACTAGCAACTG-3′ and reverse 5′-CGCTCTCGATTGCCACCTAC-3′; GAPDH, forward 5-AGCCACATCGCTCAGACAC-3′ and reverse 5′-GCCCAATACGACCAAATCC-3′. All PCR reactions were performed in triplicates.

Immunoprecipitation and Western blotting

Nuclear extracts (NEs) were prepared from cultured cells, and immunoprecipitation and Western blotting were performed as previously described (Lu *et al.*, 2014). Briefly, NEs were incubated

FIGURE 5: HEXIM1 is required for the assembly of P-TEFb into the 7SK snRNP. (A, B) Nuclear extracts (NE) were prepared from control or HEXIM1 KD MDA-MB-231, A, or F1C2, B, cells and subjected to immunoprecipitation with anti-CDK9 or anti-FLAG antibodies. The 7SK snRNP, SEC, and BRD4 associations were examined by Western blotting. (C) CDK9 was isolated from control or HEXIM1 KD F1C2 cells with anti-FLAG, and CDK9-associated proteins were visualized by silver staining. (D) Control or HEXIM1 KD MDA-MB-231 cells were treated with 0.05 μM GA for 24 h. Binding of CDK9 to Hsp90 and HEXIM1 was analyzed by immunoprecipitation with anti-CDK9 followed by Western blotting. (E) CDK9, CycT1, and Hsp90 exist in the same complex. F1C2 HEXIM1 KD cells expressing HA-Hsp90 were subjected to sequential immunoprecipitation: first with anti-FLAG antibody (for CDK9-FLAG) and then with anti-HA. CycT1 that associates with both CDK9 and Hsp90 was detected by Western blotting. (F) In vitro kinase assays. The free P-TEFb was isolated from the F1C2 nuclear extract by immunoprecipitation with anti-FLAG under the high-salt condition (1 M KCl + 1% NP-40). The Hsp90-associated P-TEFb was isolated with anti-HA-Hsp90 from HEXIM1 KD F1C2 cells. The CDK9 levels in the two complexes were normalized before the complexes were subjected to an in vitro kinase assay. p-CTD^{52}, phospho-CDK9 (p-CDK9), CDK9, CycT1, and Hsp90 were detected by Western blotting. (G) F1C2 cells were treated for 24 h with varying concentrations of GA as indicated. CDK9 was isolated from NE by immunoprecipitation with anti-FLAG, and CDK9-associated proteins were detected by Western blotting with the indicated antibodies for the 7SK snRNP, SEC, and BRD4 complexes. (H, I) Clonogenic growth of breast cancer cells was inhibited by iCDK9 treatment either alone, H, or together with GA, I. Data are presented as means ± SD in triplicates. *$p < 0.05$, **$p < 0.01$, Student's *t* test. (J) A model of HEXIM1 function in P-TEFb maturation and processing. CDK9–CycT1–Hsp90 and CDK9–CycT1–HEXIM1 complexes are necessary intermediates that allow transfer of CDK9 from Hsp90 to the 7SK snRNP.

with specific antibodies coupled to protein A beads at 4°C for from 2 h to overnight. After being washed with buffer D (20 mM HEPES-KOH, pH 7.9, 15% glycerol, 0.2 mM EDTA, 0.1% NP-40, 1 mM DTT, and 0.5 mM PMSF) containing 0.3 M KCl, the proteins of interest were eluted with 0.1 M glycine (pH 2.0) and analyzed by Western blotting with the indicated antibodies.

In vitro kinase assay

The P-TEFb complexes were isolated by immunoprecipitation, and the immune complex immobilized on antibody beads was incubated with 100 ng GST-CTD[52] at 30°C for 30 min in a 25-μl reaction buffer containing 10 mM $MgCl_2$, 50 mM NaCl, 50 mM HEPES pH 7.4, 1 mM DTT, and ±50 μM ATP. The kinase reaction was stopped by the addition of 10 μl of 4× SDS loading buffer and boiled at 95°C for 10 min.

Three-dimensional culture

Culture of mammary epithelial cells in the 3D laminin-rich extracellular matrix (Matrigel) was done as described previously (He *et al.*, 2008). Briefly, cells were seeded in growth factor–reduced Matrigel (BD Biosciences) in the wells in an eight-well chamber slide and fed every 4 days. Drug treatment was performed at day 4. Cells were fixed on day 7 and stained for α6-integrin as a basal–lateral marker. Microscopy was performed on a Zeiss LSM710 confocal microscope at the Berkeley Biological Imaging Facility.

Wound healing assay and cell migration

Cells were cultured in 12-well plates to confluence. A plastic tip was used to generate a wound across the cell monolayer. The wound closure was measured after 24 h. Migration assays were performed in Transwell chambers (Corning). In medium containing 1% FBS, 1×10^5 cells were seeded onto membranes in top chambers and allowed to migrate toward the bottom chambers filled with medium containing 10% FBS. Migrated cells were stained with 0.1% crystal violet in methanol.

The soft agar assay

Five thousand cells were suspended in 1.2 ml medium containing 0.375% Bacto Agar (BD) and overlaid on the hardened bottom layer containing 0.66% agar in a well of a six-well plate. Fresh medium (1.2 ml) containing 0.375% agar was added to each well once a week for 3 wk. The colonies were visualized by staining with 0.5 mg/ml 3-(4,5-dimethylthiazol-2-yl)-2,5-diphenyl tetrazolium bromide (MTT) (Sigma) for 4 h at 37°C.

Proliferation, colony formation, and survival assays

Thirty thousand cells were seeded in triplicate in six-well plates for 24 h and treated with drugs or DMSO at varying concentrations. Proliferation of cells were scored by cell counting at day 3–5 and normalized to the control DMSO-treated group. For colony formation assay, 1×10^3 cells were seeded in a well in 6-well plates in triplicates for 24 h and treated with drugs. Cell colonies were fixed with 4% paraformaldehyde for 10 min and stained with 0.1% crystal violet for 15 min at room temperature. To evaluate apoptosis or cell survival, 1×10^6 cells were seeded in a well of six-well plates and then treated with 0.05 μM GA for an additional 48 h. Cells were stained with 50 μg/ml propidium iodide (BD, Cat# 550825) and analyzed by flow cytometry.

In vivo xenograft assay

Female nude mice (6 wks old) were obtained from Jackson Lab. MDA-MB-231 control and HEXIM1 KD cells (2×10^6 cells) were injected subcutaneously to induce tumor formation. Tumor growth was monitored by measurement of tumor diameters with a caliper, and the tumor volume was calculated using the following formula: volume = $0.52 \times (\text{length} \times \text{width}^2)$. After tumors reached a measurable size (~100 mm^3), GA (20 mg/kg) was injected intraperitoneally twice per week for three additional weeks. The solid tumors were then removed and weighed.

Histology and TUNEL assay

Tumors were fixed in 4% formalin and paraffin embedded. The embedded tissues were sectioned and stained with hematoxylin and eosin (H&E) according to a standard protocol using Shandon Gemini Varistain ES Automated Slide Stainer (Thermo Fisher Scientific). The tumor sections were subjected to the TUNEL assay using the TUNEL immunofluorescence kit (Promega) according to the manufacturer's instructions. The level of apoptosis was quantified by comparing the number of apoptotic cells to that of the total cells.

Immunohistochemistry

Immunohistochemistry was performed on a breast cancer tissue array (BR1503b, US Biomax) using the Tyramide Signal Amplification Biotin System Kit (NEL700A001KT, Akoya Biosciences) with anti-HEXIM1 antibodies (1:200, ab245494, abcam), following the manufacturer's instructions. Images were captured using the Zeiss AxioImager M1 microscope, and the relative signal intensity was quantified by ImageJ software. The average intensity per pixel was measured on each image of the stained slide.

Database analysis

We examined the expression profile of HEXIM1 in two human cancer datasets from the Cancer Genome Atlas (TCGA) (https://cancergenome.nih.gov) and Oncomine (www.oncomine.org), using the threshold search criteria as previously described (Ji *et al.*, 2014). The Mann–Whitney test was used to evaluate the significance of differences in HEXIM1 expression between the cancer and normal control groups.

Statistical analysis

Data are presented as mean values from at least three biological replicates, with error bars denoting standard deviations. Comparisons between two groups were analyzed using the two-tailed Student's *t* test. The significance level was set at *p* values $*p < 0.05$, $**p < 0.01$, $***p < 0.001$. Statistical analyses were conducted using ImageJ and the Graphpad Prism software.

ACKNOWLEDGMENTS

This study is supported by DOD/U.S. Army Medical Research and Materiel Command W81XWH-15-1-0068 to K.L. and Qiang Z. and NIH/NIAID R01 AI041757 to Qiang Z. We thank Kartoosh Heydari and the Flow Cytometry Facility at UC Berkeley for technical assistance. We thank Steve Ruzin and Denise Schichnes at the CNR biological imaging facility at UC Berkeley for operation of microscopy and assistance with IHC experiments. We also thank Armann Andaya from the Campus Mass Spectrometry Facilities at UC Davis for assistance with mass spectrometry protein identification.

REFERENCES

Andrieu G, Tran AH, Strissel KJ, Denis GV (2016). BRD4 regulates breast cancer dissemination through Jagged1/Notch1 signaling. Cancer Res 76, 6555–6567.

Beliakoff J, Bagatell R, Paine-Murrieta G, Taylor CW, Lykkesfeldt AE, Whitesell L (2003). Hormone-refractory breast cancer remains sensitive to the

antitumor activity of heat shock protein 90 inhibitors. Clin Cancer Res 9, 4961–4971.
Blobel GA, Kalota A, Sanchez PV, Carroll M (2011). Short hairpin RNA screen reveals bromodomain proteins as novel targets in acute myeloid leukemia. Cancer Cell 20, 287–288.
Caldas-Lopes E, Cerchietti L, Ahn JH, Clement CC, Robles AI, Rodina A, Moulick K, Taldone T, Gozman A, Guo Y, *et al.* (2009). Hsp90 inhibitor PU-H71, a multimodal inhibitor of malignancy, induces complete responses in triple-negative breast cancer models. Proc Natl Acad Sci USA 106, 8368–8373.
Calero R, Morchon E, Martinez-Argudo I, Serrano R (2017). Synergistic antitumor effect of 17AAG with the PI3K/mTOR inhibitor NVP-BEZ235 on human melanoma. Cancer Lett 406, 1–11.
Dawson MA, Prinjha RK, Dittmann A, Giotopoulos G, Bantscheff M, Chan WI, Robson SC, Chung CW, Hopf C, Savitski MM, *et al.* (2011). Inhibition of BET recruitment to chromatin as an effective treatment for MLL-fusion leukaemia. Nature 478, 529–533.
He N, Jahchan NS, Hong E, Li Q, Bayfield MA, Maraia RJ, Luo K, Zhou Q (2008). A La-related protein modulates 7SK snRNP integrity to suppress P-TEFb-dependent transcriptional elongation and tumorigenesis. Mol Cell 29, 588–599.
He N, Liu M, Hsu J, Xue Y, Chou S, Burlingame A, Krogan NJ, Alber T, Zhou Q (2010). HIV-1 Tat and host AFF4 recruit two transcription elongation factors into a bifunctional complex for coordinated activation of HIV-1 transcription. Mol Cell 38, 428–438.
Jang MK, Mochizuki K, Zhou M, Jeong HS, Brady JN, Ozato K (2005). The bromodomain protein Brd4 is a positive regulatory component of P-TEFb and stimulates RNA polymerase II-dependent transcription. Mol Cell 19, 523–534.
Jeronimo C, Forget D, Bouchard A, Li Q, Chua G, Poitras C, Therien C, Bergeron D, Bourassa S, Greenblatt J, *et al.* (2007). Systematic analysis of the protein interaction network for the human transcription machinery reveals the identity of the 7SK capping enzyme. Mol Cell 27, 262–274.
Ji X, Lu H, Zhou Q, Luo K (2014). LARP7 suppresses P-TEFb activity to inhibit breast cancer progression and metastasis. Elife 3, e02907.
Ketchart W, Ogba N, Kresak A, Albert JM, Pink JJ, Montano MM (2011). HEXIM1 is a critical determinant of the response to tamoxifen. Oncogene 30, 3563–3569.
Ketchart W, Smith KM, Krupka T, Wittmann BM, Hu Y, Rayman PA, Doughman YQ, Albert JM, Bai X, Finke JH, *et al.* (2013). Inhibition of metastasis by HEXIM1 through effects on cell invasion and angiogenesis. Oncogene 32, 3829–3839.
Krueger BJ, Jeronimo C, Roy BB, Bouchard A, Barrandon C, Byers SA, Searcey CE, Cooper JJ, Bensaude O, Cohen EA, *et al.* (2008). LARP7 is a stable component of the 7SK snRNP while P-TEFb, HEXIM1 and hnRNP A1 are reversibly associated. Nucleic Acids Res 36, 2219–2229.
Lin C, Smith ER, Takahashi H, Lai KC, Martin-Brown S, Florens L, Washburn MP, Conaway JW, Conaway RC, Shilatifard A (2010). AFF4, a component of the ELL/P-TEFb elongation complex and a shared subunit of MLL chimeras, can link transcription elongation to leukemia. Mol Cell 37, 429–437.
Lu H, Li Z, Xue Y, Schulze-Gahmen U, Johnson JR, Krogan NJ, Alber T, Zhou Q (2014). AFF1 is a ubiquitous P-TEFb partner to enable Tat extraction of P-TEFb from 7SK snRNP and formation of SECs for HIV transactivation. Proc Natl Acad Sci USA 111, E15–E24.
Lu H, Xue Y, Yu GK, Arias C, Lin J, Fong S, Faure M, Weisburd B, Ji X, Mercier A, *et al.* (2015). Compensatory induction of MYC expression by sustained CDK9 inhibition via a BRD4-dependent mechanism. Elife 4, e06535.
Mbofung RM, McKenzie JA, Malu S, Zhang M, Peng W, Liu C, Kuiatse I, Tieu T, Williams L, Devi S, *et al.* (2017). HSP90 inhibition enhances cancer immunotherapy by upregulating interferon response genes. Nat Commun 8, 451.
Michels AA, Fraldi A, Li Q, Adamson TE, Bonnet F, Nguyen VT, Sedore SC, Price JP, Price DH, Lania L, *et al.* (2004). Binding of the 7SK snRNA turns the HEXIM1 protein into a P-TEFb (CDK9/cyclin T) inhibitor. EMBO J 23, 2608–2619.
Morchikh M, Cribier A, Raffel R, Amraoui S, Cau J, Severac D, Dubois E, Schwartz O, Bennasser Y, Benkirane M (2017). HEXIM1 and NEAT1 long non-coding RNA form a multi-subunit complex that regulates DNA-mediated innate immune response. Mol Cell 67, 387–399.e385.
Mori Y, Sato F, Selaru FM, Olaru A, Perry K, Kimos MC, Tamura G, Matsubara N, Wang S, Xu Y, *et al.* (2002). Instabilotyping reveals unique mutational spectra in microsatellite-unstable gastric cancers. Cancer Res 62, 3641–3645.
Mueller D, Garcia-Cuellar MP, Bach C, Buhl S, Maethner E, Slany RK (2009). Misguided transcriptional elongation causes mixed lineage leukemia. PLoS Biol 7, e1000249.
O'Keeffe B, Fong Y, Chen D, Zhou S, Zhou Q (2000). Requirement for a kinase-specific chaperone pathway in the production of a Cdk9/cyclin T1 heterodimer responsible for P-TEFb-mediated tat stimulation of HIV-1 transcription. J Biol Chem 275, 279–287.
Ogba N, Doughman YQ, Chaplin LJ, Hu Y, Gargesha M, Watanabe M, Montano MM (2010). HEXIM1 modulates vascular endothelial growth factor expression and function in breast epithelial cells and mammary gland. Oncogene 29, 3639–3649.
Ott M, Geyer M, Zhou Q (2011). The control of HIV transcription: keeping RNA polymerase II on track. Cell Host Microbe 10, 426–435.
Ouchida R, Kusuhara M, Shimizu N, Hisada T, Makino Y, Morimoto C, Handa H, Ohsuzu F, Tanaka H (2003). Suppression of NF-kappaB-dependent gene expression by a hexamethylene bisacetamide-inducible protein HEXIM1 in human vascular smooth muscle cells. Genes Cells 8, 95–107.
Paraiso KH, Haarberg HE, Wood E, Rebecca VW, Chen YA, Xiang Y, Ribas A, Lo RS, Weber JS, Sondak VK, *et al.* (2012). The HSP90 inhibitor XL888 overcomes BRAF inhibitor resistance mediated through diverse mechanisms. Clin Cancer Res 18, 2502–2514.
Ren C, Zhang G, Han F, Fu S, Cao Y, Zhang F, Zhang Q, Meslamani J, Xu Y, Ji D, *et al.* (2018). Spatially constrained tandem bromodomain inhibition bolsters sustained repression of BRD4 transcriptional activity for TNBC cell growth. Proc Natl Acad Sci USA 115, 7949–7954.
Shi J, Wang Y, Zeng L, Wu Y, Deng J, Zhang Q, Lin Y, Li J, Kang T, Tao M, *et al.* (2014). Disrupting the interaction of BRD4 with diacetylated Twist suppresses tumorigenesis in basal-like breast cancer. Cancer Cell 25, 210–225.
Sidera K, Patsavoudi E (2014). HSP90 inhibitors: current development and potential in cancer therapy. Recent Pat Anticancer Drug Discov 9, 1–20.
Smyth T, Paraiso KHT, Hearn K, Rodriguez-Lopez AM, Munck JM, Haarberg HE, Sondak VK, Thompson NT, Azab M, Lyons JF, *et al.* (2014). Inhibition of HSP90 by AT13387 delays the emergence of resistance to BRAF inhibitors and overcomes resistance to dual BRAF and MEK inhibition in melanoma models. Mol Cancer Ther 13, 2793–2804.
Sobhian B, Laguette N, Yatim A, Nakamura M, Levy Y, Kiernan R, Benkirane M (2010). HIV-1 Tat assembles a multifunctional transcription elongation complex and stably associates with the 7SK snRNP. Mol Cell 38, 439–451.
Solit DB, Osman I, Polsky D, Panageas KS, Daud A, Goydos JS, Teitcher J, Wolchok JD, Germino FJ, Krown SE, *et al.* (2008). Phase II trial of 17-allylamino-17-demethoxygeldanamycin in patients with metastatic melanoma. Clin Cancer Res 14, 8302–8307.
Suzuki Y, Kondo Y, Hara S, Kimata R, Nishimura T (2010). Effect of the hsp90 inhibitor geldanamycin on androgen response of prostate cancer under hypoxic conditions. Int J Urol 17, 281–285.
Tan JL, Fogley RD, Flynn RA, Ablain J, Yang S, Saint-Andre V, Fan ZP, Do BT, Laga AC, Fujinaga K, *et al.* (2016). Stress from nucleotide depletion activates the transcriptional regulator HEXIM1 to suppress melanoma. Mol Cell 62, 34–46.
Wedeh G, Cerny-Reiterer S, Eisenwort G, Herrmann H, Blatt K, Hadzijusufovic E, Sadovnik I, Mullauer L, Schwaab J, Hoffmann T, *et al.* (2015). Identification of bromodomain-containing protein-4 as a novel marker and epigenetic target in mast cell leukemia. Leukemia 29, 2230–2237.
Whitesell L, Lindquist SL (2005). HSP90 and the chaperoning of cancer. Nat Rev Cancer 5, 761–772.
Winter GE, Rix U, Carlson SM, Gleixner KV, Grebien F, Gridling M, Muller AC, Breitwieser FP, Bilban M, Colinge J, *et al.* (2012). Systems-pharmacology dissection of a drug synergy in imatinib-resistant CML. Nat Chem Biol 8, 905–912.
Wittmann BM, Wang N, Montano MM (2003). Identification of a novel inhibitor of breast cell growth that is down-regulated by estrogens and decreased in breast tumors. Cancer Res 63, 5151–5158.
Xue Y, Yang Z, Chen R, Zhou Q (2010). A capping-independent function of MePCE in stabilizing 7SK snRNA and facilitating the assembly of 7SK snRNP. Nucleic Acids Res 38, 360–369.
Yang Z, Yik JH, Chen R, He N, Jang MK, Ozato K, Zhou Q (2005). Recruitment of P-TEFb for stimulation of transcriptional elongation by the bromodomain protein Brd4. Mol Cell 19, 535–545.
Yang Z, Zhu Q, Luo K, Zhou Q (2001). The 7SK small nuclear RNA inhibits the CDK9/cyclin T1 kinase to control transcription. Nature 414, 317–322.

Yeramian A, Vea A, Benitez S, Ribera J, Domingo M, Santacana M, Martinez M, Maiques O, Valls J, Dolcet X, *et al.* (2016). 2-phenylethynesulphonamide (PFT-mu) enhances the anticancer effect of the novel hsp90 inhibitor NVP-AUY922 in melanoma, by reducing GSH levels. Pigment Cell Melanoma Res 29, 352–371.

Yik JH, Chen R, Nishimura R, Jennings JL, Link AJ, Zhou Q (2003). Inhibition of P-TEFb (CDK9/Cyclin T) kinase and RNA polymerase II transcription by the coordinated actions of HEXIM1 and 7SK snRNA. Mol Cell 12, 971–982.

Yokoyama A, Lin M, Naresh A, Kitabayashi I, Cleary ML (2010). A higher-order complex containing AF4 and ENL family proteins with P-TEFb facilitates oncogenic and physiologic MLL-dependent transcription. Cancer Cell 17, 198–212.

Zhou Q, Li T, Price DH (2012). RNA polymerase II elongation control. Annu Rev Biochem 81, 119–143.

Zhou Q, Yik JH (2006). The yin and yang of P-TEFb regulation: implications for human immunodeficiency virus gene expression and global control of cell growth and differentiation. Microbiol Mol Biol Rev 70, 646–659.

Zhu Q, Krakowski AR, Dunham EE, Wang L, Bandyopadhyay A, Berdeaux R, Martin GS, Sun L, Luo K (2007). Dual role of SnoN in mammalian tumorigenesis. Mol Cell Biol 27, 324–339.

Zuber J, Shi J, Wang E, Rappaport AR, Herrmann H, Sison EA, Magoon D, Qi J, Blatt K, Wunderlich M, *et al.* (2011). RNAi screen identifies Brd4 as a therapeutic target in acute myeloid leukaemia. Nature 478, 524–528.